

A Frequency-Selective Nested Dual-Loop Broadband Low-Noise Amplifier in 90 nm CMOS

Sumit Bagga^{*†}, Andre L. Mansano^{*}, Wouter A. Serdijn^{*}, John R. Long^{*}, Kathleen Philips[‡] and John J. Pekarik[§]

^{*}ERL/DIMES, Delft University of Technology, 2628 CD Delft, The Netherlands

E-mail: sumit.bagga@ieee.org, {a.l.mansano, w.a.serdijn and j.r.long}@tudelft.nl

[†]DFchip, Centro de Apoio ao Desenvolvimento Tecnológico (CDT), Brasília-DF, Brazil

[‡]IMEC-NL, Holst Centre, 5605 KN Eindhoven, The Netherlands

[§]IBM Microelectronics, Essex Junction, Vermont 05452, USA

Abstract—A broadband, frequency-selective low-noise amplifier (LNA) with at least 25 dB of rejection at frequencies below the L-band (includes GPS and GSM carriers) is fabricated in a 90 nm standard CMOS process. The proposed LNA can be used for broadband impulse-radio ultra-wideband (IR-UWB) and frequency modulated FM-UWB. The frequency-selective (3.5-10.5 GHz) LNA is power-to-current (P-I) configured and comprises nested reactive feedback loops: a positive current-to-current (I-I) feedback loop to boost the power gain and a negative I-I feedback loop for impedance and noise matching. The measured gain of the P-I LNA is 15 ± 3 dB. It has a noise figure (NF) of 2.4 ± 0.8 dB and a 1-dB gain compression point ($P_{-1\text{dB}}$) of -17.5 ± 2.5 dBm. The die area of the LNA is 0.7×0.8 mm² and it consumes 9.6 mW from a 0.8 V power supply. The proposed P-I LNA is most suitable for a sub-1 V single-cell radios.

I. INTRODUCTION

Broadband wireless systems transmitting at low power spectral densities tend to overlap and share bandwidth with existing narrowband systems. Narrowband interference (NBI) mitigation remains unresolved, as existing solutions are too complex or are ineffective in rejecting narrowband interferers [1]. Recent studies show that non-coherent type receivers are especially vulnerable to NBI. For a non-coherent auto-correlation receiver (ACR), the narrowband interference term, $i(t)$ may be defined as

$$i(t) = \mu^{(ii)} + \mu^{(in)} + \mu^{(is)}, \quad (1)$$

where $\mu^{(ii)}$, $\mu^{(in)}$ and $\mu^{(is)}$ are the interference-interference, interference-noise and interference-signal correlation terms, respectively [1]. Through digital signal processing, $\mu^{(ii)}$ can be reduced by several orders of magnitude. However, terms $\mu^{(in)}$ and $\mu^{(is)}$ may not be completely removed. These unwanted interference terms must be suppressed in the analog RF front-end to limit bit-error-rate (BER) degradation. The average bit-error probability (BEP) of an ACR with and without a notch (of bandwidth B_{NF}) is shown in Fig. 1 for different values of the signal-to-interference ratio (SIR), $C/I = E_b/(T_b P_i)$, where T_b is the bit duration, E_b is the energy per bit of the signal, and P_i is the power of the narrowband interferer. NBI is modeled by a single tone sinusoidal interferer.

For practical reasons, a passive filter (as designed in [2]) is often placed at the RF input of the receiver's front-end in order to reject out-of-band interferers. The drawback with this

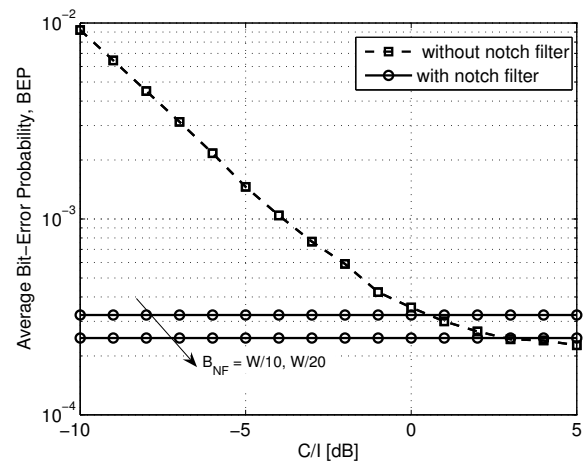


Fig. 1. Simulated average BEP of an auto-correlation receiver with and without a rectangular notch filter of bandwidth, B_{NF} , where W is approximately 2 GHz.

approach is that the insertion loss of passive filters adds to the overall noise figure of the receiver. An alternative solution is to distribute the required interference rejection in the RF front-end by means of a notch antenna that offers attenuation in the passband [3] in conjunction with a frequency-selective broadband amplifier designed to reject out-of-band signals. The frequency-selective LNA is the topic of this work. The P-I LNA is based on [4].

The next section begins with a brief discussion on single and dual-loop feedback systems, followed by a detailed description of the proposed LNA (Section II). Measurement results are presented and compared to recently published results in Section III.

II. LNA WITH NESTED REACTIVE FEEDBACK

A. Single and Dual Feedback Loops

Negative feedback promotes insensitivity to process and supply variations, stabilization of gain, lower distortion, larger bandwidth (at the expense of gain), and orthogonal noise and impedance matching [5] in broadband amplifiers. In principle, a single current-to-current (I-I) negative feedback loop together with a transistor's transconductance, g_m , can define its input impedance. Due to the limited loop-gain at

higher frequencies, and to facilitate the trade-off between impedance matching and gain, a second positive feedback loop is introduced (as in [4]). A power-to-current (P-I) configuration is the preferred choice, as the proposed LNA is to be interfaced with a mixer or an IF filter.

B. P-I LNA with Negative I-I and Positive I-I Feedback

Fig. 2 shows the topology of the frequency-selective P-I LNA. The frequency-selective P-I LNA comprises a single common-source stage (M_1), and two reactive networks made up of current-to-current transformers (T_1 in concentric configuration with weak mutual coupling and T_2 in stacked configuration with strong mutual coupling) followed by a common-gate stage (M_2). Transistor M_2 with the reactive feedback networks forms a high impedance output node. To keep the noise figure to a minimum while maintaining sufficiently high gain, the LNA is biased (using bias-T networks) between optimum noise and f_T points.

With the intermediate I-I positive feedback loop (as shown in Fig. 2), the input impedance (Z_i) is made less susceptible to the turns ratio and coupling coefficient of the gain boosting transformer. To maintain stability, the carefully controlled positive feedback loop must be stabilized by the negative (balancing) feedback loop. This loop works as follows: the output current (i_o) at the primary winding Lp_2 of T_2 is sensed and added to the drain current (i_x) of M_1 , thereby boosting the transconductance of the first stage ($G_m \triangleq i_o/v_i$) without increasing the bias current or the aspect ratio. For the negative feedback loop (as in [2]), the output current (and not the intermediate current, i_x) is sensed by the primary winding Lp_1 of T_1 and added to the gate of the common-source stage M_1 . This facilitates the trade-off in gain and impedance matching. Inductance L_3 resonates with the parasitic capacitances of M_2 (provides gain peaking) to compensate for the high frequency gain roll-off. The bondwires and bondpads are modeled using L_B and C_B , respectively.

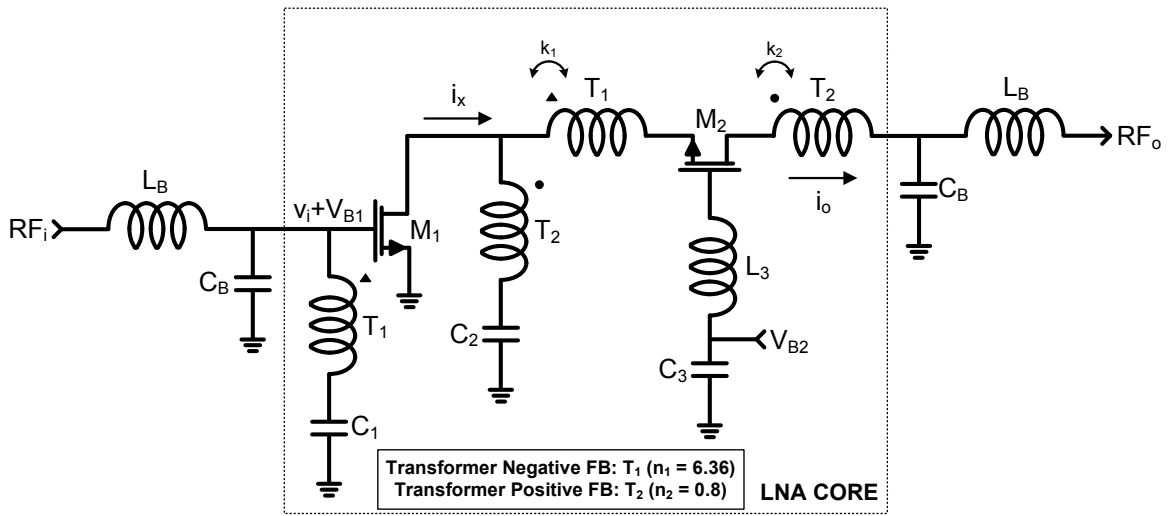


Fig. 2. Schematic of the frequency-selective P-I LNA with nested (negative and positive I-I) reactive feedback loops.

Transformer non-idealities are neglected to simplify the analysis. The role of the positive feedback transformer, T_2 is to provide additional current gain, which in turn boosts the transconductance of the first stage, g_m to G_m (Fig. 3), thereby increasing the power gain and sets Z_i to 50Ω (4).

$$G_m = \frac{g_m}{1 - (k_2/n_2)} \quad (2)$$

where k_2 is the coupling coefficient and n_2 is the turns ratio of transformer T_2 .

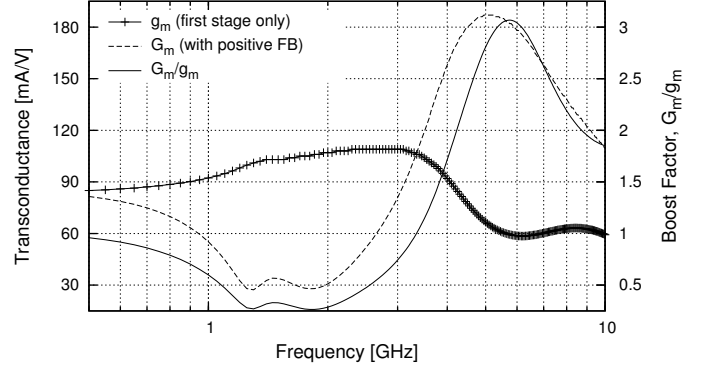


Fig. 3. Transconductance boosting with a positive I-I feedback loop.

The power gain is expressed as,

$$G_p = A_i G_m Z_L = \left(\frac{n_1}{k_1} \right) \left(\frac{g_m}{1 - (k_2/n_2)} \right) Z_L \quad (3)$$

where A_i is the current gain of the LNA, k_1 is the coupling coefficient and n_1 is the turns ratio of transformer T_1 , and Z_L is the load impedance.

From the individual loop equations, the input impedance (Z_i) can be expressed as,

$$Z_i = \frac{A_i}{G_m} = \left(\frac{n_1}{k_1} \right) \left(\frac{1 - (k_2/n_2)}{g_m} \right) \quad (4)$$

The second feedback loop (i.e., variable k_2/n_2) allows for more control over the input impedance.

To realize a power gain ≥ 14 dB, an input impedance of 50Ω and a noise figure ≤ 3 dB, the transformer parameters presented in Table I are used.

TABLE I
CONCENTRIC AND STACKED TRANSFORMER PARAMETERS

Trans.	k	L_s (nH)	L_p (nH)	N^\dagger	$Q_{s/p}^\ddagger$	OD (mm ²)
T_1	0.3	2.1	0.33	8.4	23/19	250x325
T_2	0.65	1.2	1.5	1.4	21/18	225x225

† Physical turns ratio, $N = (n/k) = \frac{\sqrt{L_s/L_p}}{k}$.
 ‡ Q-factor of T_1 and T_2 simulated at 6.5 GHz.

The broadband notch in the stopband is a result of the series LC resonant network formed with the secondary winding, L_{s1} of T_1 and AC coupling capacitor C_1 .

III. MEASUREMENT RESULTS

The microphotograph of the fabricated P-I LNA is shown in Fig. 4. The chip area is 0.56 mm^2 ($0.7 \times 0.8 \text{ mm}^2$) including bondpads. The active area is approximately 0.3 mm^2 . All inductors, transformers and metal-insulator-metal (MiM) capacitors are implemented in the top two thick metallization layers. The windings of the non-inverting transformers, T_1 and T_2 are concentric and stacked, respectively.

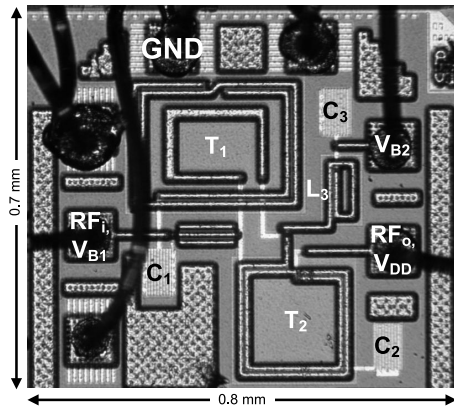


Fig. 4. Microphotograph of the frequency-selective P-I LNA in 90 nm CMOS.

The measured and simulated results for the forward transmission (S_{21}) and reflection (S_{11}) coefficients are shown in Fig. 5. In the passband (3.5-10.5 GHz), the power gain is 15 ± 3 dB. The LNA presents 30 dB of rejection at frequencies below the L-band (includes GPS and GSM carriers). The transconductance of the cascode and the transformer parameters, such as the self-inductances of the windings, physical turns ratio and coupling coefficient, set the input impedance of the LNA (Fig. 5). An acceptable S_{11} over a broad frequency range is ≤ -10 dB. The measured S_{11} varies from -7 to -16 dB.

A linear phase (or uniform group delay) response is paramount in broadband amplifier design. The measured phase response (of the S_{21}) of the P-I LNA is shown in Fig. 6. At

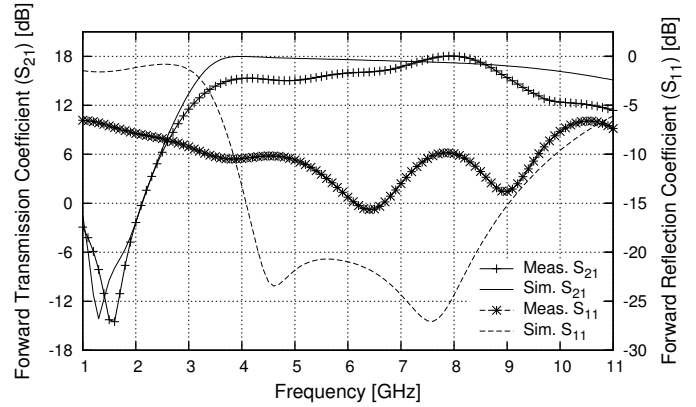


Fig. 5. Forward transmission and reflection coefficients of the P-I LNA (after de-embedding). Gain peaking is from 7 to 9 GHz instead of 8 to 10 GHz as a result of larger self-inductance of L_3 .

the resonance frequency, the LNA demonstrates a phase jump of approximately 125 degrees. The group delay (including the test fixture) is approximately 330 ± 40 ps across the passband.

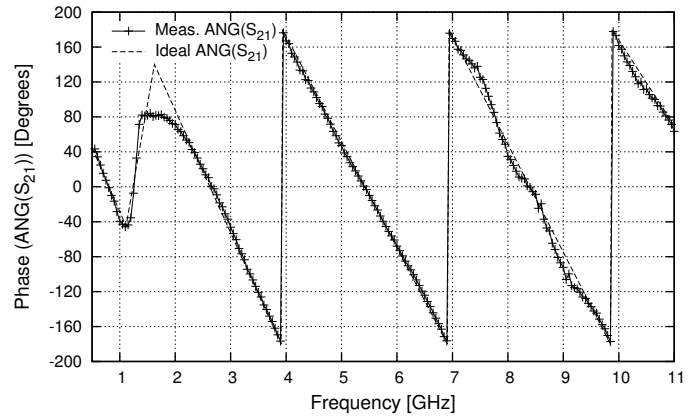


Fig. 6. Phase response of the P-I LNA (including the test fixture).

The measured reverse transmission coefficient (isolation), $S_{12} \leq -20$ dB ($\Delta 10$ dB from simulated) is shown in Fig. 7. Discrepancy in S_{12} is a result of unwanted parasitic feedback.

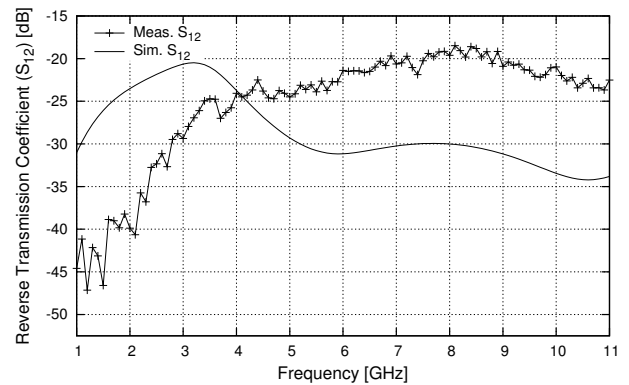


Fig. 7. Reverse transmission coefficient of the P-I LNA.

TABLE II
SUMMARY OF THE P-I LNA AND COMPARISON WITH PREVIOUSLY PUBLISHED DESIGNS

Specifications	This work	[6]	[7]	[8]	[9]	[10]	[11]	[12]
BW (GHz)	3.5-9.25	3.25-10.25	3.1-10.6	3.0-10	2.4-9.5	3-10	3.4-11.4	0.2-5.2
S ₂₁ (dB)	15±3	14.5±2.5	15.3±2.2	19±2	7.8±1.5	18.5±1.7	14.75±1.25	15.6*
Notch (dB)	≥ 30 [§]	≥ 20 [†]	n.a.	n.a.	n.a.	n.a.	n.a.	n.a.
S ₁₁ (dB)	(-16) to (-8)	(-16) to (-10.5)	(-25) to (-8.6)	(-14) to (-9)	(-38) to (-15)	< -7.2	(-40) to (-10)	< -10
S ₁₂ (dB)	< -20	< -36	< -25	n.a.	< -35	< -37	< -45	n.a.
GD (ps)	330±40	225±125	102.5±27.5	n.a.	187.5±62.5	n.a.	n.a.	n.a.
NF (dB)	2.4±0.8	2.9±0.8	2.51±0.47	3.4±0.85	6.6±2.6	2.45±0.65	4.55±1.45	< 3.5
IIP3 (dBm)	(-10) to (-5) [‡]	(-9) to (-1.8)	(-7.2) to (-4.3)	(-5.5) to 3	(-8.2) to (-5.6)	2.1 (6 GHz)	-7 (6 GHz)	> 0
V _{DD} /P (V/mW)	0.8/9.6	1.2/15	1.2/9	3.3/30	1.8/9	3.3/26	1.8/11.9	1.2/21
Area (mm ²)	0.56	1.68	0.87	1.8	1.1	0.72	1.2	0.009
Tech. (nm)	C-90	C-130	C-130	SiGe-180	C-180	SiGe-180	C-180	C-65

*Voltage gain; [§]Measured @ 1.5 GHz; [†]Measured @ 5.25 GHz; [‡]Extrapolated IIP3 (i.e., measured P_{-1dB} + 9.6 dB).

The noise figure (2.4±0.8 dB) is plotted in Fig. 8. As the transformer coupling degrades at lower frequencies, the noise figure is higher. At higher frequencies, the noise figure is greater because of more substrate and parasitic losses. In broadband amplifier design, reactive feedback increases linearity without increasing thermal noise. It is often the case that linearity of an amplifier deteriorates as frequency increases, however, in transformer-based feedback systems, the effects are not as profound. The 1-dB compression point, P_{-1dB} (-17±2.5 dBm) is an appropriate measure of the linearity for broadband circuits (see Fig. 8). The input-inferred third-order intercept point (IIP3) can be extrapolated from the P_{-1dB}.

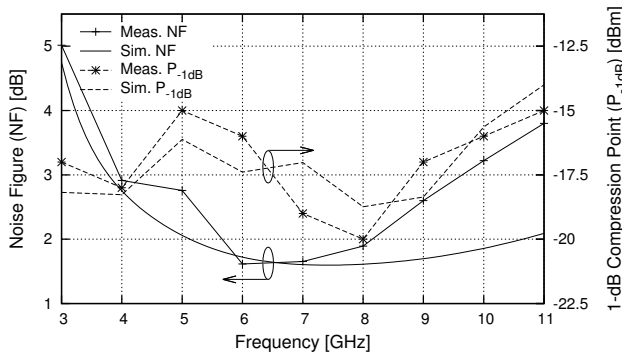


Fig. 8. Noise figure and 1-dB compression point of the P-I LNA.

Table II compares the frequency selective P-I LNA to recently published wideband LNAs in standard CMOS and SiGe HBT technologies. This prototype demonstrates superior design characteristics, such as a smaller silicon footprint, capacity to operate from a lower voltage supply, is least technology dependent (as a result of feedback) and provides excellent out-of-band rejection.

IV. CONCLUSION

A g_m -boosted frequency-selective LNA with nested reactive feedback loops in 90 nm standard CMOS is presented. Reactive feedback loops are constructed using on-chip concentric and stacked current-to-current transformers. A broadband notch is placed in the stopband to suppress narrowband

interferers below the L-band (includes GSM carriers). The measured power gain of the LNA is 15±3 dB. The noise figure (2.4 dB) and the 1-dB compression point (-17.5 dBm) exhibit a 0.8 dB and 2.5 dBm variation across the passband. Total power dissipation is 9.6 mW from a 0.8 V supply. This LNA is intended for sub-1 V single-cell radios.

V. ACKNOWLEDGMENT

The authors gratefully acknowledge technical and financial support provided by TUD, The Netherlands and CNPq, Brazil.

REFERENCES

- [1] S. Bagga, *Ultra-wideband Transceiver Circuits and Systems*, Ph.D. thesis, Delft University of Technology, Delft, The Netherlands, 2009.
- [2] S. Bagga, Z. Irahauten, W. A. Serdijn, J. R. Long, and J. Pekarik, "An UWB transformer-c orthonormal state space band-reject filter in 0.13 μm CMOS," *IEEE European Solid-State Circuits Conference*, pp. 298–301, Sept. 2008.
- [3] H. G. Schantz, G. Wolenc, and E. M. Myszkla III, "Frequency notched UWB antennas," *IEEE Conference on Ultra Wideband Systems and Technologies*, pp. 214–218, Nov. 2003.
- [4] S. Bagga, "Dual-Loop Feedback Amplifying Circuit," *United States Patent*, no. US2011/0148527, June 2011.
- [5] X. Li and W. A. Serdijn, "On the design of broadband power-to-current low noise amplifiers," *IEEE Transactions on Circuits and Systems I*, vol. 59, no. 3, pp. 493–504, Mar. 2012.
- [6] S. Bagga, Z. Irahauten, W. A. Serdijn, J. R. Long, J. Pekarik, and Hans Pflug, "A band-reject ir-UWB LNA with 20 dB WLAN suppression in 0.13 μm CMOS," *IEEE Asian Solid-State Circuits Conference*, pp. 449–452, Nov. 2008.
- [7] M. T. Reiha and J. R. Long, "A 1.2 V reactive-feedback 3.1-10.6 GHz ultra-wideband low-noise amplifier in 0.13 μm CMOS," *IEEE Journal of Solid-State Circuits*, pp. 1023–1033, May 2007.
- [8] A. Ismail and A.A. Abidi, "A 3.1-10.6 GHz low-noise amplifier with wideband LC-ladder matching network," *IEEE Journal of Solid-State Circuits*, vol. 39, no. 12, pp. 2269–2277, Dec. 2004.
- [9] A. Bevilacqua and A.M. Niknejad, "An ultra-wideband CMOS low-noise amplifier for 3.1-10.6 GHz wireless receivers," *IEEE Journal of Solid-State Circuits*, vol. 39, no. 12, pp. 2259–2268, Dec. 2004.
- [10] Y. Lu, R. Krithivasan, W.-M. L. Kuo, and J. D. Cressler, "A 1.8-3.1 dB noise figure (3-10 GHz) SiGe HBT LNA for UWB applications," *IEEE Radio Frequency Integrated Circuits (RFIC) Symposium*, pp. 59–62, June 2006.
- [11] Y.-J. Lin, S. S. H. Hsu, J.-D. Jin, and C. Y. Chan, "A 3.1-10.6 GHz ultra-wideband CMOS low noise amplifier with current-reused technique," *Microwave and Wireless Component Letters*, pp. 232–234, Mar. 2007.
- [12] S. C. Blaakmeer, E. A. M. Klumperink, D. M. W. Leenaerts, and B. Nauta, "Wideband Balun-LNA with Simultaneous Output Balancing, Noise-Canceling and Distortion-Canceling," *IEEE Journal of Solid-State Circuits*, vol. 43, no. 6, pp. 1341–1350, June 2008.